ITPK1 sensitizes tumor cells to IgA-dependent neutrophil killing in vivo

Richterich, C.A.; Logtenberg, M.E.W.; Jansen, M.J.H.; Toebes, M.; Bresser, K.; Borst, A.; ... ; Schumacher, T.N.

ITPK1 Sensitizes Tumor Cells to IgA-dependent Neutrophil Killing In Vivo

Connor A Richterich, Meike E W Logtenberg, Marco J H Jansen, Mireille Toebes, Kaspar Bresser, Anne Borst, Anouk P Jurgens, Jeanette H W Leusen, Ton N Schumacher

ITPK1 Sensitizes Tumor Cells to IgA-dependent Neutrophil Killing In Vivo

Connor A. Richterich,*,†,1 Meike E. W. Logtenberg,*,†,1 Marco J. H. Jansen,‡,1 Mireille Toebes,* Kaspar Bresser,†,§,¶ Anne Borst,* Anouk P. Jurgens,†,§,¶ Jeanette H. W. Leusen,‡,2 and Ton N. Schumacher*,†,‖,2

Neutrophils can efficiently trigger cytotoxicity toward tumor cells and other target cells upon engagement of the IgA receptor CD89. However, the cell-intrinsic factors that influence the induction of cell death upon exposure to neutrophil effector mechanisms in vivo remain largely unknown. To uncover genetic regulators that influence target cell sensitivity to IgA-induced neutrophil-mediated killing, we used a human CD89 (hCD89) transgenic mouse model in which IgA-mediated killing of Her2-positive CD47-deficient murine target cells is mediated by neutrophils. Using a genome-wide in vivo screening approach, we demonstrate that deletion of the gene encoding inositol-tetrakisphosphate 1 kinase (ITPK1) increases survival of target cells in anti-Her2 IgA-treated mice. Moreover, we show that this effect depends on neutrophil activity and on the ITPK1 kinase domain. Notably, ITPK1 deficiency did not measurably impact survival of IgA-opsonized target cells in in vitro systems, underscoring the importance of in vivo screening systems to uncover physiologically relevant regulators of neutrophil killing. ***The Journal of Immunology*****, 2024, 213: 1244–1254.**

Tumor-targeting Abs, including the Her2-specific Abs trastuzumab and margetuximab and the CD20-specific Abs rituximab and ofatumumab, can direct the cytotoxic mechanisms of immune cells toward opsonized cancer cells via their Fc domains (1–6). The tumor-targeting Abs in current clinical use all carry the IgG isotype Fc domain that, depending on the specific subclass, engage immune cells expressing activating Fcγ receptors (FcγRs), in particular macrophages and NK cells. More recently, tumor-targeting Abs containing the IgA isotype Fc domain have been proposed as an alternative to IgG Abs to specifically engage immune cells expressing the IgA receptor (CD89 or FcαRI) and thereby make use of their unique effector functions. CD89 is highly expressed on neutrophils (7), with more limited expression on macrophages and monocytes (8, 9). In addition, prior work has demonstrated that IgA Abs are superior to IgG Abs in their capacity to induce neutrophil activation and swarming (7, 10). Thus, IgA-based neutrophil engagers may potentially exhibit antitumor activity in cancer types in which IgG-based therapies have been less effective.

Neutrophils are the most abundant leukocytes in circulating blood and indispensable for both the clearance of microbial infections and wound healing (11). In cancer, neutrophils have been shown to display both pro- and antitumor activities, with antitumor activities presumed to dominate when neutrophils are triggered through ITAM receptors, such as the activating FcγRs and CD89 (7). In this work, we aimed to uncover determinants of tumor cell sensitivity to neutrophil-mediated killing. The mechanisms that control the functional outcome of ITAM receptor signaling in different myeloid and lymphoid cell types follow a shared logic, and prior analyses of cellular determinants that control T cell function therefore form a useful paradigm for mechanisms that may control neutrophil function. Specifically, research over the past years has identified three broad classes of tumor cell determinants that influence tumor cell killing by cytotoxic T cells. First, a series of mutations have been identified that interfere with Ag presentation, including disruption of genes encoding the TAP transporter and β_2-microglobulin, thereby preventing the initial event of ITAM receptor (i.e., TCR) signaling (12). Second, (over-)expression of ligands for ITIM receptors, such as programmed death-ligand 1 (PD-L1) by tumor cells, has been shown to reduce T cell effector functions even when Ag is presented (13). Finally, a third class of resistance mechanisms is exemplified by overexpression of the granzyme B inhibitor SERPINB9. In this case, proximal and downstream T cell activation are both unaffected, but the cytotoxic consequence of the resulting T cell degranulation event is reduced (14). Similar to T cell–target cell interactions, neutrophils also form immunological synapses with opsonized target cells when engaging Ag via their Fc receptors (15). Furthermore, analogous to

*Division of Molecular Oncology & Immunology, Oncode Institute, The Netherlands Cancer Institute, Amsterdam, the Netherlands; †Oncode Institute, Utrecht, the Netherlands; ‡Laboratory for Translational Immunology, UMC Utrecht, Utrecht, the Netherlands; §Department of Hematopoiesis, Sanquin Research, Amsterdam, the Netherlands; ¶Landsteiner Laboratory (AMC), Amsterdam UMC, Amsterdam, the Netherlands; and ‖Department of Hematology, Leiden University Medical Center, Leiden, the Netherlands

[1]These authors contributed equally to this work.

[2]These authors contributed equally to this work.

ORCIDs: 0009-0004-0954-284X (C.A.R.); 0000-0002-8981-1189 (M.E.W.L.); 0000-0001-9545-2023 (M.T.); 0000-0001-7113-0476 (K.B.); 0000-0003-0813-0689 (A.B.); 0000-0003-4982-6914 (J.H.W.L.); 0000-0003-0517-8804 (T.N.S.).

Received for publication May 31, 2023. Accepted for publication August 9, 2024.

This work was supported by the Stevin award and the Louis Jeantet http://dx.doi.org/10.13039/501100001706 prize (to T.N.S.) and by SENSIT (Grant agreement 742259).

The deep sequencing data presented in this article have been submitted to the National Center for Biotechnology Information Gene Expression Omnibus (https://www.ncbi.nlm.nih.gov/geo/query/acc.cgi?acc=GSE273588) under accession number GSE273588.

Address correspondence and reprint requests to Prof. Ton N. Schumacher, Netherlands Cancer Institute, Plesmanlaan 121, 1066 CX Amsterdam, Noord-Holland, the Netherlands. E-mail address: t.schumacher@nki.nl

The online version of this article contains supplemental material.

Abbreviations used in this article: CFP, cyan fluorescent protein; CT, CellTrace; FcγR, Fcγ receptor; FERMT3, FERM domain containing integrin activator kindlin 3; IPMK, inositol polyphosphate multikinase; ITPK1, inositol-tetrakisphosphate 1 kinase; KO, knockout; MLKL, mixed lineage kinase domain-like; OE, overexpression; PD-L1, programmed death-ligand 1; WT, wild type.

https://doi.org/10.4049/jimmunol.2300372

the effect of PD-L1–PD-1 interactions on T cell activation, (over-) expression of CD47, a ligand for the SIRPα ITIM receptor that is expressed on neutrophils, has been shown to interfere with neutrophil effector functions upon recognition of opsonized target cells (16–18). However, intracellular determinants that influence tumor cell sensitivity to neutrophil effector functions, analogous to the protective effect of SERPINB9 against T cell–derived granzyme B, have to date not been described.

In this study, we identify inositol-tetrakisphosphate 1 kinase (ITPK1), a cytosolic kinase that can generate higher-order inositol phosphates, as a positive regulator of tumor cell sensitivity toward in vivo killing using a genome-wide in vivo CRISPR screening approach. Furthermore, we show that this phenotype relies on an intact ITPK1 kinase domain, and we provide evidence of an epistatic relationship between ITPK1 and inositol polyphosphate multikinase (IPMK). Finally, we demonstrate that although neutrophils form the dominant selective pressure in vivo, the effects of ITPK1 deletion are not observed in in vitro target cell killing assays, thereby underpinning the value of in vivo screening approaches to study neutrophil-mediated tumor cell control.

Materials and Methods

Mice

Hemizygous hCD89-transgenic mice (19, 20) backcrossed to the BALB/cByJRj background were maintained as described (10), and transgene negative littermates were used as control animals. Note that there is no known mouse homolog of the CD89 gene. All mice were housed and bred at Janvier Labs, Paris, France, or at Utrecht University. Mice were randomized based on age, sex, and genotype, and, upon transfer to Utrecht, mice were acclimatized for at least 1 wk prior to the start of experiments. Animal experiments were carried out in compliance with the relevant ethical regulations and approved by the Instantie voor Dierenwelzijn committee (AVD115002016410; Utrecht, The Netherlands).

Vector generation

The coding sequence of human Her2 (hHer2) was obtained by restriction digest using the EcoRI and NotI sites in a pMX-puromycin-N-acetyltransferase vector encoding hHer2 (21). The coding sequence of the human CD19 (hCD19, UniProt identifier P15391) extracellular and transmembrane domain with an N-terminal P2A element was ordered as a codon-optimized gene fragment (IDT DNA). The pMX vector encoding hHer2 and hCD19, separated by a P2A sequence (pMX-fhHer2-P2A-thCD19), was created using Gibson assembly (22), and inserts were validated by Sanger sequencing.

To generate the focused sgRNA library, 2 sgRNAs for each gene selected in the primary screen, together with 10 nontargeting control sgRNAs, were picked. For each sgRNA, a forward and reverse orientation single-stranded DNA oligonucleotide was generated (Thermo Fisher), based on the 20-base sgRNA sequence and the corresponding overhangs produced by the BsmB1 restriction enzyme. Next, oligonucleotide pairs were annealed in T4 ligation buffer (New England Biolabs, B0202S) at a concentration of 10 μM, by heating to 95°C and subsequently cooling to 25°C in a ramp-down period of 45 min. Next, annealed oligonucleotides were pooled and diluted to a final concentration of 0.2 μM. A golden-gate reaction mixture was generated by mixing 1 μL of the oligo pool with 20 ng lenti-Guide-Puro vector (Addgene 52963), 1 μL of BsmBI-v2 (New England Biolabs R0739S), 1 μl T4 ligase (New England Biolabs, M0202S), and T4 ligase buffer (New England Biolabs, B0202S) in a final volume of 50 μl. The resulting mixture was incubated in a thermocycler for 15 cycles of 5 min at 37°C and 20 min at 20°C. Next, 2 μl of the golden gate reaction mixture was used for transformation of Endura Electrocompetent cells (Lucigen, 60242). The sgRNA representation in the resulting plasmid library was analyzed using the MiSeq platform (Illumina).

The coding sequences of murine ITPK1 (mITPK1, UniProt identifier Q8BYN3) and mITPK1 D295A were ordered as codon-optimized gene fragments (Twist Biosciences) and inserted into the EcoRI and NotI sites of the retroviral pMX-mCherry vector. The coding sequence for murine CD47 (UniProt Identifier Q61735) was ordered as codon-optimized clonal vector (pTwist Lenti SFFV Puro WPRE, Twist Biosciences).

Cell lines

Unless indicated otherwise, the immortalized pro-B cell line Ba/F3 overexpressing hCD19, hHer2, Cas9, and GFP and deficient for CD47, hereafter termed "sensBa/F3," was used as a target cell line sensitive to neutrophil killing. To generate sensBa/F3 cells, Ba/F3 cells (23) were retrovirally transduced with the pMX-fhHer2-P2A-thCD19 vector, and cells expressing hHer2 and hCD19 were isolated using FACS. Next, Cas9 was introduced by means of retroviral transduction with pCas9-GFP (Addgene, 44719), and a clonal cell line was obtained for subsequent modifications. To generate CD47-deficient cells, this cell line was electroporated with a pLentiCRISPR-v2 (Addgene, 52961) plasmid DNA encoding an sgRNA targeting murine CD47. The electroporated cells were subsequently selected for 48 h with 10 μg/ml puromycin and, after selection, a single-cell clone deficient for CD47 was obtained, thereby yielding the sensBa/F3 target cell line.

To obtain cyan fluorescent protein (CFP)-positive target cells, sensBa/F3 cells were retrovirally transduced with the pMX-CFP vector and subsequently enriched via FACS. To obtain CFP-Katushka double-positive target cells, sensBa/F3 cells expressing CFP were retrovirally transduced with the pMX-Katushka vector and subsequently enriched via FACS.

To generate ITPK1 knockout (KO) cell lines, sensBa/F3 cells were transduced with the lenti-Guide-Puro vector (Addgene 52963) encoding an ITPK1-specific sgRNA (5′-GTTCGAACGGCCAAGCGATG-3′). Control cells were produced using the lenti-Guide-Puro (Addgene, 52963) vector encoding a nontargeting sgRNA sequence (5′-GTAGTGCGTGTGATGTC GGG-3′). Following transduction, cells were cultured for 7 d in the presence of 5 μg/ml puromycin, and surviving cells were expanded to obtain bulk populations. Next, single cells were isolated and expanded to obtain clonal KO populations, termed "sensBa/F3 sgITPK1." Gene disruption was validated by sequence analysis of the ITPK1 gene locus using TIDE (24) and Western blot analysis.

To generate wild-type (WT) and ITPK1 D295A overexpressing cells, sensBa/F3 sgITPK1 cells were retrovirally transduced with a pMX-mCherry vector encoding either the WT murine ITPK1 protein or the D295A mutated ITPK1 protein. Subsequently, mCherry-positive cells were enriched using FACS, and ITPK1 overexpression (OE) was confirmed by Western blot analysis. The resulting cell lines were termed "sensBa/F3 sg ITPK1" and "ITPK1 OE" or "sensBa/F3 sg ITPK1" and "ITPK1^{D295A} OE," respectively. To genetically reconstitute CD47, sensBa/F3 (i.e., CD47-deficient, hHer2-positive) cells were lentivirally transduced with a vector encoding the murine CD47 sequence, and cells expressing CD47 were selected using FACS.

All cells were cultured at 37°C and 5% CO_2 in RPMI (Thermo Fisher, 11875093) supplemented with 10% (v/v) FCS (Thermo Fisher, 26140079), penicillin-streptomycin (Thermo Fisher, 15140148) and 0.2 ng/ml recombinant murine IL-3 (Immunotools, 12340032).

Flow cytometry

The following Abs were used: anti-hHer2 (BioLegend, 324405 or 324407, clone 24D2, dilution 1:100–200), anti-hCD19 (BioLegend, 302201 or 302211, clone HIB19, dilution 1:100–200), anti-mouse CD47 (BioLegend, 127501, clone miap301, dilution 1:100–200), anti-mouse CD11b (BioLegend, 101207 or 101219, clone M1/70, dilution 1:500), anti-mouse F4/80 (Bio Legend, 123115 or 123141 or 123117, clone BM8, dilution 1:200), anti-mouse Gr-1 (Thermo Fisher 25-5931-82, clone RB6-8C5, dilution 1:400), and anti-mouse Ly-6G (BioLegend, 127601 or 127617 or 127641, clone 1A8, dilution 1:400).

For flow cytometric analysis of cells grown in vitro, cells were washed in PBS containing 0.5% (w/v) BSA (Sigma-Aldrich, A7030) and 0.2% (w/v) sodium azide (Sigma-Aldrich, S2002) (FACS buffer) and stained with the indicated Abs in FACS buffer for 20–30 min at 4°C while protected from light. Subsequently, cells were washed with FACS buffer, and DAPI or propidium iodide was added to allow for dead cell exclusion.

For flow cytometric analysis of Ba/F3 and effector cells retrieved from the peritoneum of mice, cells were incubated with 5% normal mouse serum for 45 min at 4–7°C. Next, cells were stained with the indicated Abs for 45–60 min at 4–7°C and subsequently washed with FACS buffer. Measurements were performed on an LSR II, LSRFortessa, or FACSCanto II (BD Biosciences), and data analysis was performed using FACSDiva (BD Biosciences) or FlowJo software (FlowJo LLC). Manual gating strategies involved a morphological gate and doublet exclusion gate based on forward and side scatter, followed by dead-cell exclusion based on the aforementioned viability dyes. Events were assigned to specific cell populations as per the indicated dyes and fluorochromes described previously. Sulfate latex beads were gated as suggested by the manufacturer's instructions.

Pooled CRISPR Cas9 in vivo genetic screens

For the genome-wide screen, sensBa/F3 cells were lentivirally transduced with the pooled Brie CRISPR KO library (Addgene, 73632/3) in the

lenti-Guide-Puro (Addgene, 52963) vector at a transduction rate of ~50% and a coverage >1800-fold. For the focused screen, sensBa/F3 cells were lentivirally transduced with the focused sgRNA library in the lenti-Guide-Puro vector (Addgene, 52963) at a transduction rate of ~50% and a coverage >2000-fold. The focused library targets 35 genes with two sgRNAs each, and with target genes selected on the basis of observed enrichment scores in the primary screen (Supplemental Fig. 2A) and RNA expression levels (Supplemental Fig. 2B). In addition, high scoring genes encoding certain transcription factors (e.g., Rhox11 and Gtf2e2) were excluded, and a number of presumed interactors of top-scoring genes (i.e., Kctd10, Cul3, and Wipf2 with Itsn2) were included (25, 26). Following transduction, the cells were cultured for >7 d in the presence of 5 μg/ml puromycin. Before injection into mice, a library reference sample was taken. Next, hCD89-transgenic mice and littermate control animals were injected i.p. with 2×10^7 cells in 200 μl PBS. Directly after target cell injection, mice received PBS (control treatment) or 100 μg anti-hHer2 IgA1 Ab in PBS by i.p. injection. At 16 h after injection, mice were euthanized, and the peritoneal cavity was washed with PBS containing 5 mM EDTA to obtain target cells and murine immune cell infiltrates. To estimate target cell killing efficiency by flow cytometry, a small aliquot was taken from each sample and pooled per treatment group (PBS or anti-hHer2 IgA1). Next, cells were stained with allophycocyanin-conjugated anti-hHer2 and anti-hCD19 Abs, and target cells were positively selected for by MACS using anti-allophycocyanin magnetic beads (Miltenyi Biotec, 130-090-855), according to the manufacturer's protocol. Thereafter, DNA was isolated from enriched target cells using the DNeasy Blood & Tissue Kit (QIAGEN, 69504). In the genome-wide screen, —three or four samples within each group were pooled on the basis of recovered DNA amounts, yielding three anti-hHer2-treated samples and three PBS-treated genomic DNA samples. Similarly, in the focused screen, two of the DNA samples derived from the treated group were pooled. sgRNA sequences in the pooled or unpooled sample groups were amplified using NEBNext High-Fidelity 2× PCR Master Mix (New England Biolabs, M0541S), following the manufacturer's instructions and using primers containing sample barcodes. After PCR, prepared libraries were pooled at equimolar amounts, and sgRNA distributions were analyzed by deep sequencing using the Illumina HiSeq2500 platform. In brief, sequence reads were aligned to the Brie mouse library, reads containing mismatches were removed, sgRNA distributions were quantified, and genes were scored using MAGeCK RRA (version 0.5.6) (27). Downstream analysis was focused on the two anti-hHer2-treated sample groups that displayed the most profound difference in sgRNA abundance compared with the PBS-treated control groups (selected mice) (Supplemental Fig. 2A), as opposed to all mice (Supplemental Fig. 2A, 2D).

Pooled CRISPR Cas9 in vivo epistasis screen

A set of 76 genes involved in cell death processes was assembled on the basis of literature research, including gene ontology terms related to apoptosis, necroptosis, ferroptosis, pyroptosis, and TNF-mediated cell death (28, 29). Furthermore, genes reported to be involved in cytokine-induced cell death were included (30). An sgRNA library targeting these 76 genes (three sgRNAs per gene) was ordered as an oligonucleotide pool (IDT DNA) and cloned into the lenti-Guide-Puro vector (Addgene, 52963). sgRNA sequences were picked using CRISPick (Broad Institute GPP Webportal). To generate sensBa/F3 cells deficient of ITPK1, sensBa/F3 cells were electroporated (Lonza, V4XP-3024) (Program E0-117) with sgRNA targeting ITPK1 (in lenti-Guide-Puro; Addgene, 52963) and selected for 48 h in 10 μg/ml puromycin. Next, single-cell clones were screened for ITPK1 inactivation by DNA sequencing and Western blot analysis, as well as for lentiviral integration. Six clones with ITPK1 deletions but without lentiviral integration were pooled. Subsequently, both sensBa/F3 cells and sensBa/F3 ITPK1 KO cells were transduced with the sgRNA library targeting the 76 cell death–related genes. Next, the resulting sensBa/F3 and sensBa/F3 ITPK1 KO cell death libraries were cultured for 10 d to remove cells containing KOs of essential genes, and sgRNA distributions were assessed using Illumina MiSeq sequencing.

The expanded sensBa/F3 cell death libraries were subsequently stained with CellTrace (CT) violet or yellow (Thermo Fisher, C34554), respectively, and pooled at a 1:1 ratio. Thereafter, the stained cell pool was i.p. injected into hCD89-transgenic mice (n = 8, 20 million cells each) that were subsequently treated with anti-hHer2 IgA or PBS (n = 4 each). After 16 h, mice were sacrificed, and cells were obtained by i.p. lavage and stained with the Near-IR Dead Cell Staining Kit (Thermo Fisher, L10119). Subsequently, viable tumor cells obtained from each mouse were sorted into CT violet– and yellow-positive populations. Next, genomic DNA of each sample was obtained using DirectPCR Lysis reagent (Viagen Biotech, 301-C) according to the manufacturer's instructions. sgRNA sequences were subsequently amplified using NebNext High-Fidelity 2× PCR Master Mix (New England Biolabs, M0541S) following the manufacturer's instructions using primers containing sample barcodes. After PCR, prepared libraries were pooled at equimolar amounts, and sgRNA library distributions were analyzed by Illumina MiSeq sequencing. In brief, sequence reads were aligned to a reference library, reads containing mismatches were removed, and sgRNA distributions were quantified and scored using MAGeCK RRA (version 0.5.6) (27). Downstream analysis focused on comparison of the positive $\log_2$ fold changes of sgRNAs between treated and untreated mice in either ITPK1-proficient or -deficient backgrounds.

Western blot analysis

For Western blot analysis, equal numbers of cells for each sample were washed in PBS and lysed in radioimmunoprecipitation assay buffer (1% Triton, 0.1% sodium deoxycholate, 0.1% SDS, 1 mM EDTA, 10 mM Tris, pH 8.0, 140 mM NaCl) containing protease inhibitors (Roche, 11697498001) and 1 mM PMSF (Sigma-Aldrich, 10837091001). After a 30-min incubation on ice, cell lysates were centrifuged at 13,300 × g for 10 min at 4°C. Supernatants were subsequently processed, and protein concentrations were measured using the Pierce BCA Protein Assay kit according to the manufacturer's instructions (Thermo Fisher, 23225). Equal amounts of protein were subsequently processed using the NuPAGE Electrophoresis system (Thermo Fisher, NP0321) and Trans-Blot Turbo Transfer system (Bio-Rad Laboratories) according to the manufacturers' instructions. ITPK1 expression was evaluated using rabbit anti-mITPK1 (Cell Signaling Technology, 96006, 1:1000 dilution) and goat anti-rabbit HRP-conjugated Ab (Thermo Fisher, 31460, 1:10000 dilution). Rabbit anti-cyclophilin-B D1V5J (Cell Signaling Technology, 43603, 1:1000 dilution) was used as a loading control.

In vivo killing assays

The peritoneal Ba/F3 tumor model in hCD89-transgenic mice (19) and in vivo competitive killing assay were used as described previously (21) or as indicated in the figure legends. In brief, Ba/F3 target cells with the genotypes of interest were labeled with the indicated CT dyes (Thermo Fisher, C34554) and pooled in PBS at equal ratios or at the ratios indicated in the corresponding figure legends. Labeling of cells with CT red, CT violet, CT yellow, and CT CFSE was performed at concentrations of 0.5 μM, 0.4–10 μM, 0.625 μM, and 1–1.25 μM, respectively, for 15 min at room temperature in PBS. Next, cell mixtures were injected into the i.p. cavity of hCD89-transgenic mice and littermate control animals. Directly after target cell injection, mice received either PBS (control treatment) or 100 μg anti-hHer2 IgA1 Ab in PBS by i.p. injection. Where indicated, mice were treated with 100 μg anti-hHer2 IgG1 (Herceptin, Roche) or anti-FITC IgG2a (Absolute Antibody, Ab00102-2.0). After 16 h or as otherwise indicated in the figure legends, mice were euthanized, and the peritoneal cavity was washed with PBS containing 5 mM EDTA to obtain target cells and murine immune cells. Subsequently, the absolute number of each target cell type was determined by flow cytometry using TruCount tubes (BD Biosciences, 340334). Abundance of indicated immune cell types in the peritoneum was measured by staining with the Abs indicated, and cell numbers were quantified relative to sulfate latex beads by flow cytometry (Thermo Fisher, S37225). To assess opsonization potential of target cells, a small sample was taken from the lavage of PBS-treated mice, and cells were incubated with anti-hHer2 IgA prior to anti-hIgA (SouthernBiotech, 2052-09) staining and FACS analysis (Supplemental Fig. 4A). To assess in vivo opsonization of target cells, a sample was taken from the lavage of anti-hHer2-treated mice and stained with anti-hIgA prior to FACS analysis (Supplemental Fig. 4B). When indicated in the figure legends, neutrophils were depleted by i.p. injection with 100 μg mouse anti-Ly-6G IgG2a (clone 1A8, Absolute Antibody, Ab00295-2.0) 2 d prior to and on the day of tumor cell challenge. Macrophages were depleted with a single i.p. injection of 100 μl chlodronate liposomes (Liposoma C-) 6 h prior to tumor cell injection.

Neutrophil isolation

Human neutrophils were isolated from healthy donor–derived peripheral blood using the MACSxpress Neutrophil Isolation Kit (Miltenyi Biotec, 130-104-434) according to the manufacturer's recommendations.

Murine neutrophils were isolated from bone marrow as follows. Femurs and tibias were isolated and were flushed with RPMI supplemented with 10% (v/v) FCS and 2 mM penicillin-streptomycin. The suspended cells were pelleted, and RBCs were lysed using RBC lysis buffer (BioLegend, 420301) for 2 min at room temperature. Next, cells were passed through a 70-μm cell strainer (Corning, 352350), washed in MACS buffer (PBS, 0.5% BSA, 2 mM EDTA), and cell concentrations were adjusted to 10^8 cells/ml. Cells were stained with anti-mouse Ly6G-PE (BD Biosciences, 551461, clone 1A8) for 45 min at a final concentration of 4 μg/ml on ice. Next, cells were washed in MACS buffer, incubated with (20 μl per 10^7 cells) anti-PE microbeads (Miltenyi Biotec, 130-048-801) for 15 min on ice, and isolated

via MACS according to the manufacturer's instructions. The cells were used for in vitro assays directly after isolation.

In vitro killing assays

Target cells were labeled with 100 μCi ^{51}Cr (PerkinElmer, NEZ030S001MC) per 10^6 cells for at least 2 h at 37°C and 5% CO_2. Next, cells were washed three times with culture media. Bone marrow–derived murine neutrophils or peripheral blood–derived human neutrophils were mixed with chromium-labeled target cells at a 40:1 E:T ratio and treated with the Abs as specified in the figure legends. After 4 h of incubation at 37°C and 5% CO_2, supernatants were transferred to a LumaPlate (PerkinElmer, 6006633), and radioactive scintillation was measured on a β-gamma counter (PerkinElmer). Specific lysis was calculated using the following formula: [(experimental cpm − spontaneous cpm)/(total cpm − spontaneous cpm) × 100%]. The total cpm was inferred from the chromium release of labeled target cells treated with 5% Triton X-100 (Sigma-Aldrich, X100-5ML). The spontaneous cpm was inferred from the chromium release of labeled target cells, which were not treated with Abs or mixed with effector cells. All assays were performed in triplicates.

Bulk RNA sequencing

Three separate cultures of Ba/F3 cells were harvested and washed once in PBS. RNA was subsequently extracted using the RNeasy Mini Kit (Qiagen, 74004) according to the manufacturer's instructions. Samples were processed using the TruSeq Stranded mRNA Kit (Illumina, 20020594) for whole-transcriptome sequencing. Samples were multiplexed and sequenced (50 bp, single-end) on an Illumina NovaSeq 6000 system (S1 flow cell). Reads were aligned to the reference genome (GRCm38, prebuilt HISAT2 index, genome_snp_tran), and transcript counts were obtained using an in-house–generated pipeline (GenSum, https://github.com/NKI-GCF/gensum).

Statistical analysis

Data are reported as mean (± SD), and statistical significance was determined using the Student *t* test, one-way ANOVA, or two-way ANOVA, as indicated in the figure legends (GraphPad Prism version 9). All Student *t* tests were two-tailed under the assumption of equal variance between samples. All one-way ANOVA tests were corrected for multiple comparisons using statistical hypothesis testing. Differences were considered statistically significant if $p < 0.05$.

Data availability

Deep sequencing data are accessible via the National Center for Biotechnology Information Gene Expression Omnibus under accession number GSE273588.

Results

Development of an in vivo screening system to assess cancer cell sensitivity to neutrophil-mediated immune pressure

Studies over the past years have provided in vivo and, in particular, in vitro evidence (31) for a series of distinct mechanisms through which neutrophils may kill their target cells. Specifically, neutrophils have the capacity to release granules that contain cytotoxic mediators, such as defensins, myeloperoxidases, and granzyme B (32). In addition, neutrophils can produce reactive oxygen species during oxidative bursts, which in turn can interact with myeloperoxidases to form cytotoxic hypochlorous acid (33). Finally, it has been shown that neutrophils have the capacity to kill opsonized tumor cells through the induction of trogoptosis, a cell death pathway that is triggered by membrane nibbling and that is enhanced when the CD47-SIRPα signaling axis is blocked (17, 18, 21, 34). The latter process has been reported to be induced by the interaction of tumor-opsonizing IgG and IgA Abs with FcγR and FcαR, respectively, on neutrophils (7, 34).

The dominant mechanism through which neutrophils kill tumor cells in vivo is likely dependent on their polarization status and may be influenced both by tumor cell characteristics and the tumor microenvironment (11, 35). To allow the identification of tumor cell–intrinsic factors that influence neutrophil-mediated killing, we set out to develop a genetic screening system that recapitulates the interplay between tumor cells, immune cells, and the tumor microenvironment in vivo. To this end, we first determined the feasibility of identifying tumor cell genotypes that influence sensitivity to neutrophil-mediated killing in vivo. Prior work has demonstrated that activation of neutrophils upon signaling through activating FcRs is controlled by the CD47–SIRPα immune checkpoint. In line with this, CD47-positive tumor cells show a reduced sensitivity to neutrophil-mediated killing (17, 18, 21). To explore whether this known phenotype could be revealed in pooled in vivo screens, hCD89-transgenic mice were injected with mixtures of CD47-deficient and CD47-proficient hHer2-positive Ba/F3 cells at ratios of 1:500 and 1:20,000, and mice were then treated with anti-hHer2 IgA (Fig. 1A, Supplemental Fig. 1A). Consistent with prior work (18, 21), analysis of i.p. immune cells showed that anti-hHer2 IgA treatment induced a myeloid infiltrate that was dominated by neutrophils (Fig. 1B). Furthermore, anti-hHer2 IgA treatment led to a significantly decreased number of tumor cells recovered from the i.p. lavage (Fig. 1C, Supplemental Fig. 1B). Importantly, anti-hHer2 IgA treatment resulted in a substantial enrichment of CD47-positive hHer2-expressing Ba/F3 cells when present at a starting frequency of 1:500 (up to ∼14-fold enrichment in IgA-treated mice relative to control) (Fig. 1D, Supplemental Fig. 1C, 1E). To understand whether CD47-positive cells present at a lower frequency (1:20,000) could also be enriched in a reproducible manner, Ba/F3 cells derived from the i.p. lavage of IgA-treated mice were expanded in vitro and then used for a second in vivo selection round (Fig. 1A). As previously, anti-hHer2 IgA administration resulted in a considerable depletion of i.p. target cells (Fig. 1E). Moreover, dual rounds of in vivo selection resulted in a significant enrichment of CD47-positive target cells in IgA-treated mice not only when present at an initial frequency of 1:500 but also when present at an initial frequence of 1:20,000 (up to ∼17-fold) (Fig. 1F, 1G, Supplemental Fig. 1C–1F). Together, these data demonstrate the feasibility of identifying genetic modifiers of tumor cell sensitivity to neutrophil attack through in vivo genetic screening.

Genome-wide CRISPR Cas9 screen uncovers ITPK1 as negative regulator of IgA-mediated neutrophil killing in vivo

To test for genetic determinants that modulate IgA-dependent neutrophil killing through a genome-wide CRISPR Cas9 screen, we leveraged the CD47-deficient hHer2-expressing Ba/F3 cell line (Fig. 1) with the aim to maximize selective pressure. Specifically, CD47-deficient, hHer2$^+$ Ba/F3 cells were further modified to stably express Cas9 in addition to hCD19 (to allow for magnetic bead sorting), resulting in the neutrophil-sensitive cell line sensBa/F3 (CD47$^-$hHer2$^+$hCD19$^+$Cas9$^+$GFP$^+$ Ba/F3). SensBa/F3 cells were subsequently transduced with a genome-wide sgRNA library, and the resulting cell library was inoculated into the i.p. cavity of hCD89-transgenic mice and control mice (Fig. 2A). Comparison of tumor cell numbers recovered from PBS-treated control mice and anti-hHer2 IgA-treated hCD89-transgenic mice revealed a significantly higher depletion of target cells in the anti-hHer2 IgA-treated group, consistent with immune pressure (Fig. 2B). The sgRNA distribution in target cells recovered from the different groups was subsequently measured and analyzed. Specifically, using Model-based Analysis of Genome-wide CRISPR/Cas9 Knockout (MAGeCK RRA) (27), genes were assigned enrichment and depletion scores (Fig. 2C), and resulting enrichment scores were then used to design a focused subgenome library containing sgRNAs that targeted 35 depleted and enriched genes (Supplemental Fig. 2A). This focused library was subsequently used in a secondary in vivo screen that exploited the same experimental setup as the primary screen (Fig. 2A). Consistent with the primary screen, tumor cell recovery was substantially reduced in anti-hHer2 IgA-treated mice relative to control mice (Fig. 2D). Furthermore, sgRNA enrichment and

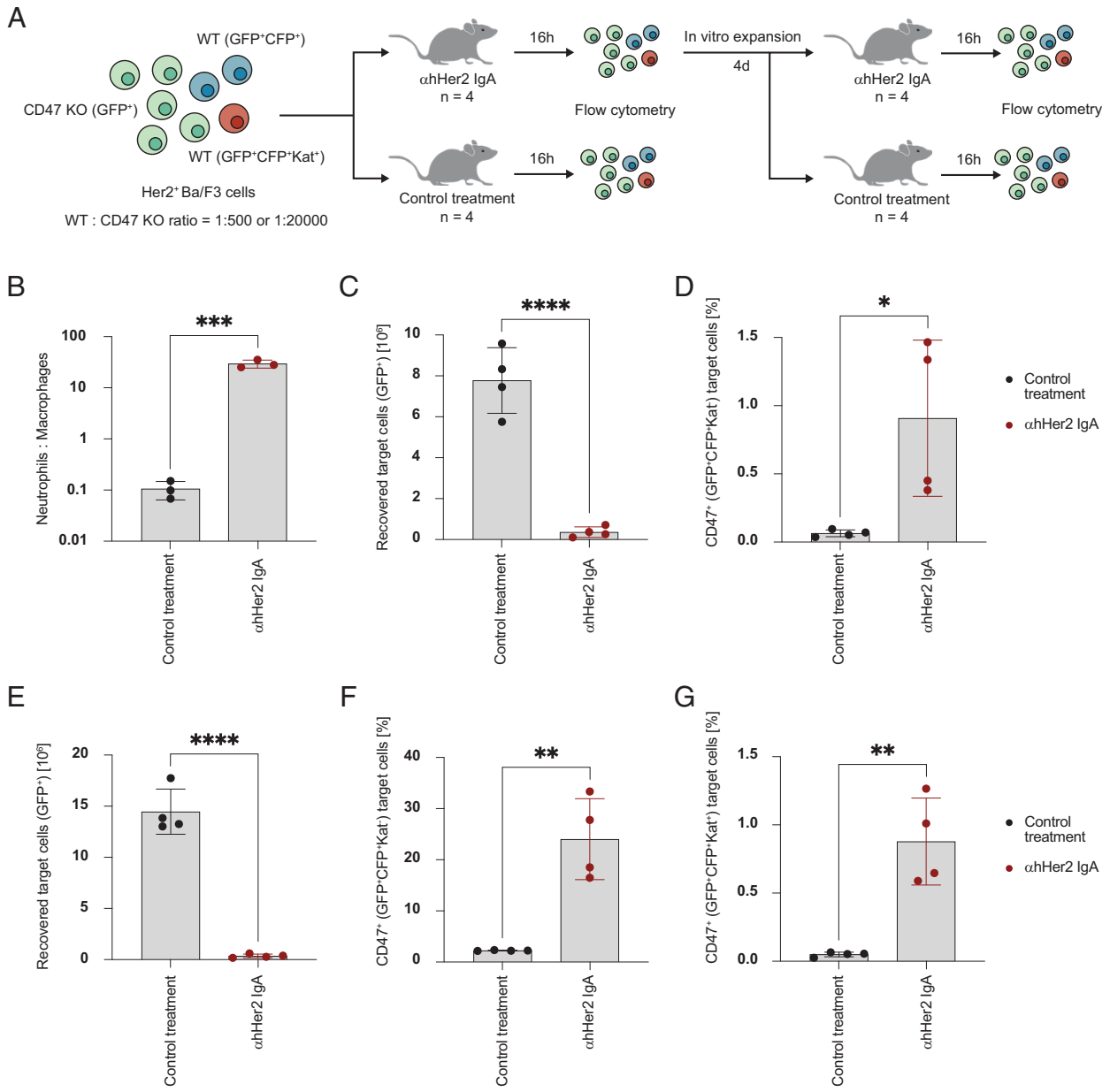

FIGURE 1. Characterization of in vivo model. (**A**) Schematic overview of experimental approach. $CD47^{+/+}$ $hHer2^{+}$ Ba/F3 tumor cells (CFP^{+} or $CFP^{+}Kat^{+}$) were mixed with $CD47^{-/-}$ $hHer2^{+}$ Ba/F3 tumor cells (GFP^{+}) in a 1:500 or 1:20,000 ratio, and 10^7 cells were injected into $hCD89^{+/-}$ transgenic mice or $hCD89^{-/-}$ littermates. The $hCD89^{+/-}$ and $hCD89^{-/-}$ mice were then treated with anti-hHer2 IgA and PBS, respectively (first selection round). After 16 h, mice were sacrificed, and tumor cells and immune cells were quantified using flow cytometry. Purified tumor cells isolated from anti-hHer2 IgA-treated mice were expanded for 4 d in vitro, and 2×10^7 cells were injected into $hCD89^{-/+}$ transgenic mice and $hCD89^{-/-}$ littermates, which were treated with anti-hHer2 IgA or PBS, respectively (second selection round). After 16 h, mice were sacrificed, and tumor cells were quantified using flow cytometry. (**B**) Ratio of neutrophils ($Ly\text{-}6G^{+}$) to macrophages ($F4/80^{+}$) recovered in the i.p. lavage of $hCD89^{+/-}$ transgenic mice and $hCD89^{-/-}$ littermates treated with anti-hHer2 IgA or PBS, respectively. Dots represent individual mice. ***$p = 0.0001$, unpaired, two-tailed t test. (**C**) Number of target cells recovered from mice treated with anti-hHer2 IgA or PBS after the first in vivo selection round. ****$p < 0.0001$, unpaired, two-tailed t test. (**D**) Fraction of $CD47^{+/+}$ CFP^{+} $Kat^{-/-}$ target cells (initially present at a 1:500 ratio) among all target cells recovered after the first in vivo selection round. Dots represent individual mice. *$p = 0.0257$, unpaired, two-tailed t test. (**E**) Number of target cells recovered from mice treated with anti-hHer2 IgA or PBS after the second in vivo selection round. Dots represent individual mice. ****$p < 0.0001$, unpaired, two-tailed t test. (**F**) Fraction of $CD47^{+/+}$ CFP^{+} $Kat^{-/-}$ target cells (initially present at a 1:500 ratio) among all target cells recovered after the second in vivo selection round. Dots represent individual mice. **$p = 0.0015$, unpaired, two-tailed t test. (**G**) Fraction of $CD47^{+/+}$ CFP^{+} Kat^{+} target cells (initially present at a 1:20,000 ratio) among all target cells recovered after the second in vivo selection round. Dots represent individual mice. **$p = 0.002$, unpaired, two-tailed t test.

depletion correlated between the primary and secondary screens (Supplemental Fig. 2A, 2C), underscoring the validity of the observed in vivo effects. Importantly, this focused screen revealed a significant enrichment of sgRNAs targeting the ITPK1 gene in IgA-treated mice (Fig. 2E, 2F), thereby uncovering ITPK1 as a potential negative regulator of IgA-mediated neutrophil killing in vivo. In addition, enrichment was also observed for sgRNAs targeting the FERM domain containing integrin activator kindlin 3 (FERMT3) (Fig. 2E).

ITPK1 deletion reduces cancer cell sensitivity to neutrophil-mediated killing in vivo but not in vitro

ITPK1 is a cytosolic kinase that can generate higher-order inositol polyphosphates (36), and this ITPK1 kinase activity has recently

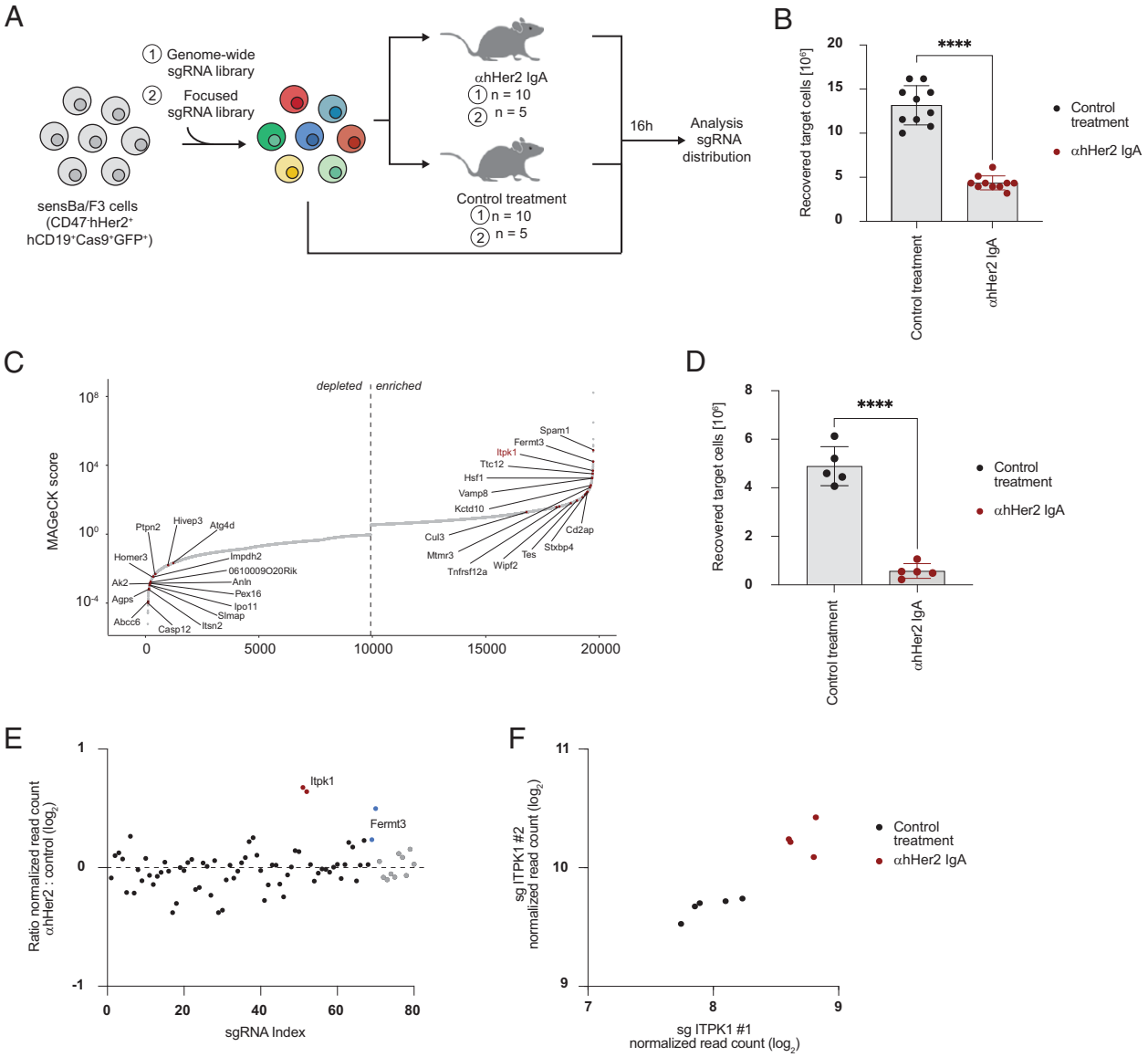

FIGURE 2. Genome-wide in vivo CRISPR Cas9 screen reveals ITPK1 as a regulator of cancer cell sensitivity to IgA-mediated killing. (**A**) Schematic overview of pooled in vivo genome-wide CRISPR Cas9 screen (1, primary screen) and pooled in vivo focused CRISPR Cas9 screen (2, secondary screen). SensBa/F3 cells were transduced with a genome-wide (1, primary screen) or focused (2, secondary screen) sgRNA library to generate KO libraries. The resulting cell libraries were subsequently injected into hCD89$^{+/-}$ transgenic mice or hCD89$^{-/-}$ littermates at 2×10^7 cells per mouse and treated with anti-hHer2 IgA or PBS, respectively. After 16 h, mice were sacrificed, genomic DNA (gDNA) was isolated from purified tumor cells, and sgRNA distributions were analyzed by deep sequencing. On the basis of observed sgRNA distributions, enrichment and depletion scores were generated using MAGeCK RRA (version 0.5.9.2). (**B**) Number of target cells isolated from mice treated with anti-hHer2 IgA or PBS in the genome-wide screen. Dots represent individual mice. ****$p < 0.0001$, unpaired, two-tailed t test. (**C**) Positive and negative MAGeCK RRA scores for each enriched and depleted gene from mice selected in primary screen. Cutoff for enrichment or depletion set at median positive RRA score. Genes contained in the focused screening library are marked in red and labeled. (**D**) Number of target cells isolated from mice treated with anti-hHer2 IgA or PBS in the focused screen. Dots represent individual mice. ****$p < 0.0001$, unpaired, two-tailed t test. (**E**) Ratio of average normalized sgRNA abundance (read counts) in tumor cells derived from anti-hHer2 IgA-treated mice versus PBS-treated mice in the focused screen. sgRNAs targeting ITPK1 are highlighted in red. sgRNAs targeting FERMT3 are highlighted in blue. Nontargeting control sgRNAs are depicted in gray. (**F**) Representation of the normalized sgRNA abundance of the two sgRNAs targeting ITPK1 in tumor cells recovered from mice treated with anti-hHer2 IgA or PBS in the focused screen. Dots represent individual mice or pooled samples as indicated in the Materials and Methods section.

been shown to be required for the execution of cytokine-induced necroptosis mediated by mixed lineage kinase domain-like (MLKL) (36). With the aim to evaluate the contribution of ITPK1 expression to neutrophil-induced tumor cell death in vitro and in vivo, we generated clonal ITPK1 KO and control sensBa/F3 cell lines with comparable hHer2 levels (Supp. Fig. 3A, 3B). Transfer of these cell lines to hCD89-transgenic mice and subsequent anti-hHer2 treatment showed that killing of sensBa/F3 cells was significantly reduced in case ITPK1 of deficiency (Fig. 3A, Supp. Fig. 3E). This reduced sensitivity of ITPK1-deficient target cells in IgA-treated mice was already visible 6 h after target cell injection and increased over time (Fig. 3C, Supp. Fig. 3C), coinciding with a substantial increase in neutrophil numbers in the intraperitoneal cavity relative to control mice at both 6 h postinjection (~12-fold), and 16 h postinjection (~16-fold) (Fig. 3B, 3D). Notably, survival of ITPK1-deficient and -proficient cells was comparable in PBS-treated control mice (Fig. 3A, 3C, Supp. Fig. 3D, 3E), thereby directly linking the observed phenotype to IgA treatment-induced immune pressure. To

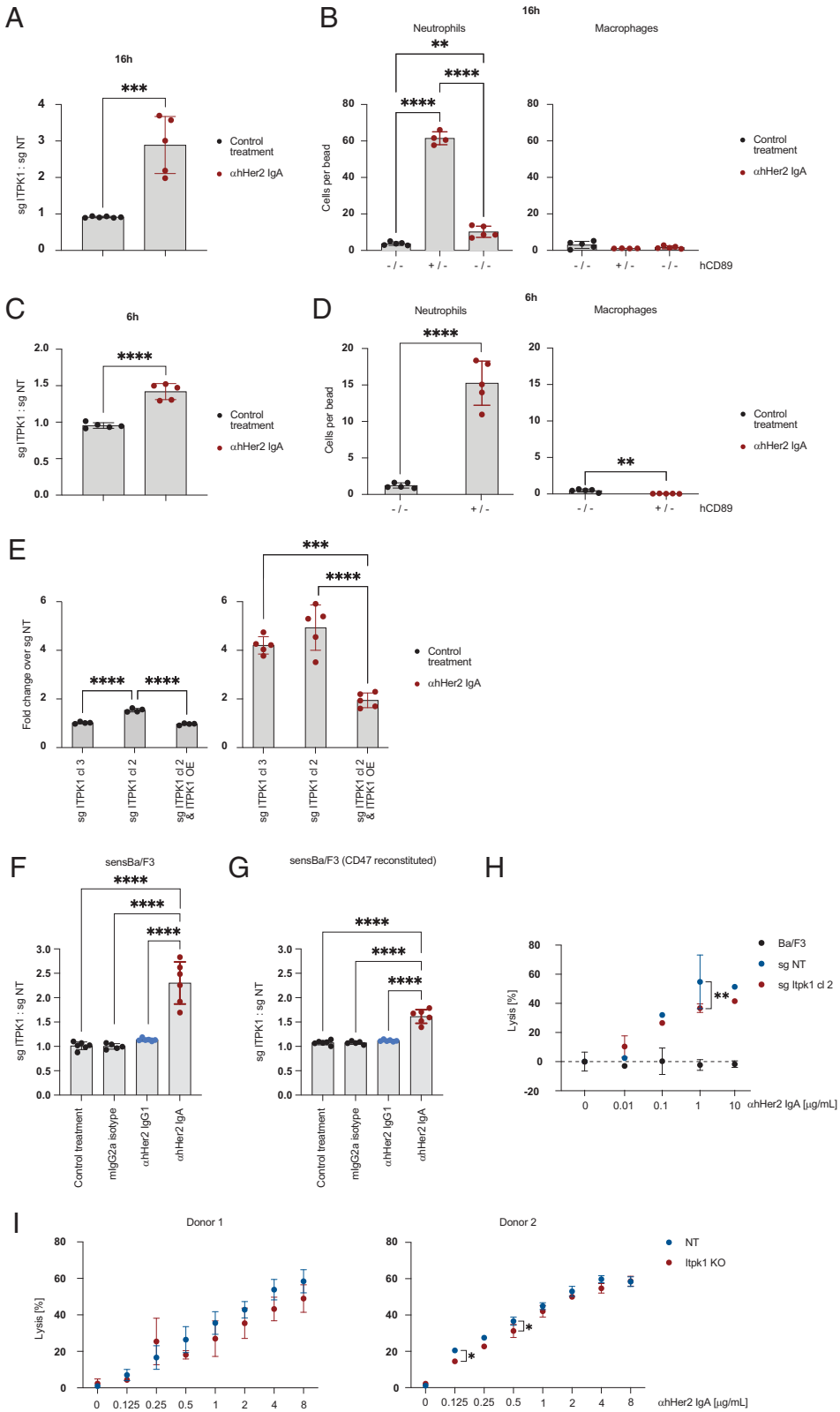

FIGURE 3. ITPK1 deletion reduces cancer cell sensitivity to IgA-mediated killing in vivo but not in vitro. (**A**) Ratio of sensBa/F3 tumor cells expressing ITPK1-targeting sgRNA (clone 2) over control cells expressing nontargeting sgRNA (NT, clone 2) recovered from hCD89$^{+/-}$ transgenic mice or hCD89$^{-/-}$ littermates after a 16-h treatment with anti-hHer2 IgA or PBS, respectively. Prior to treatment, mice were injected with an equal mixture of sensBa/F3 tumor cells with the previously indicated genotypes. Dots represent individual mice. ***$p = 0.0001$, unpaired, two-tailed t test. (**B**) Relative abundance of neutrophils (CD11b^{+}Ly6G^{+}) and macrophages (CD11b^{+}F4/80^{+}) in the i.p. lavage of hCD89$^{+/-}$ transgenic mice treated for 16 h with anti-hHer2 IgA or hCD89$^{-/-}$ littermates treated for 16 h with either anti-hHer2 IgA or PBS. Dots represent individual mice. Prior to treatment, mice were injected with an equal mixture of sensBa/F3 tumor cells expressing either ITPK1-targeting or nontargeting sgRNA. ****$p < 0.0001$, **$p = 0.007$, no indication = nonsignificant, one-way ANOVA. (**C**) Ratio of sensBa/F3 tumor cells expressing ITPK1-targeting sgRNA (clone 2) over control cells expressing nontargeting sgRNA (NT, clone 2) recovered from hCD89$^{+/-}$ transgenic mice or hCD89$^{-/-}$ littermates after a 6-h treatment with anti-hHer2 *(Figure legend continues)*

test whether the sensitivity of sensBa/F3 cells to IgA-mediated neutrophil killing could be restored, an ITPK1-deficient clone was modified to constitutively express the coding sequence of ITPK1. Overexpression of ITPK1 resensitized sensBa/F3 cells to IgA treatment-induced killing (Fig. 3E, Supp. Fig. 3F), validating ITPK1 as a sensitizer to IgA-mediated target cell killing in vivo.

Given the widespread clinical use of human IgG-based antibody therapeutics, the sensitivity of ITPK1-deficient sensBa/F3 cells to treatment with anti-hHer2 IgG1 (trastuzumab) was also evaluated. Unlike what was observed upon treatment with IgA, anti-hHer2 IgG treatment led to only subtle hHer2-dependent tumor cell clearance (Supplemental Fig. 3H). Consequently, the present data do not address whether the observed protective effect of ITPK1 deficiency upon IgA treatment extends to other Ig isotypes (Fig. 3F, Supp. Fig. 3H). Next, to evaluate whether ITPK1 expression also influences the in vivo sensitivity of CD47-proficient target cells to anti-hHer2 IgA treatment, we created ITPK1-deficient and -proficient sensBa/F3 cells with reconstituted CD47 expression and compared cell survival upon IgA treatment. Although differential survival of ITPK1-deficient relative to IPTK1-proficient cells was most prominent when CD47 was absent, ITPK1 deficiency also resulted in a modest but significant effect on IgA-dependent target cell survival in CD47-expressing cells (Fig. 3G).

Interestingly, ITPK1 deficiency did not measurably influence sensitivity to IgA-induced killing in in vitro cultures of bone marrow–derived hCD89-positive murine neutrophils with ITPK1-proficient and -deficient CD47-deficient hHer2-positive Ba/F3 cells (Fig. 3H). As a control, hHer2-deficient Ba/F3 cells did resist IgA-induced neutrophil killing in these cultures (Fig. 3H). Similarly, when coculturing hHer2-expressing K562 cells with peripheral blood–derived human neutrophils, no differential survival of ITPK1-competent and -deficient cancer cells was observed upon IgA treatment (Fig. 3I). Collectively, these data establish that ITPK1 regulates in vivo target cell sensitivity to IgA-induced killing; however, this protective effect is not detected in neutrophil-based in vitro killing assays.

ITPK1-dependent cancer cell sensitivity requires an intact ATP-binding grasp

Prior studies have shown that the aspartic acid at position 295 (D295) of ITPK1 is a crucial residue in its ATP-binding grasp and that mutations in D295 significantly compromise inositol (3–6) P_4 1-kinase activity (37, 38). To determine whether the sensitizing effect of ITPK1 on IgA-induced target cell killing is dependent on its kinase activity, we generated ITPK1-deficient sensBa/F3 cells that either overexpressed the WT coding sequence of ITPK1 or a kinase-dead (D295A) ITPK1 variant. Subsequently, hCD89-transgenic mice were i.p. injected with the resulting cell lines, along with either ITPK1-proficient or -deficient sensBa/F3 cells, and parental Ba/F3 cells (Fig. 4A). Analysis of cell recovery again showed the reduced sensitivity of ITPK1-deficient cells relative to cells endogenously expressing ITPK1 in IgA-treated mice (Fig. 4B). In contrast, overexpression of ITPK1 had a significant, yet minor, effect on target cell sensitivity in the absence of IgA treatment (Fig. 4B). Notably, although overexpression of the WT ITPK1 coding sequence restored the sensitivity of ITPK1 KO Ba/F3 cells to IgA-induced killing, such restoration was not observed upon overexpression of the kinase-dead D295A ITPK1 variant (Fig. 4B). Thus, ITPK1 functions as a sensitizer to IgA-mediated killing, but only when its ATP-binding grasp is intact.

ITPK1-dependent cancer cell sensitivity depends on neutrophils

IgA treatment results in an i.p. immune infiltrate that is composed primarily of neutrophils, and prior work has demonstrated a dominant role of neutrophils as effector cells in this model (18, 21), both suggesting that the observed phenotype of ITPK1 deficiency reflects a reduced sensitivity to neutrophil-mediated killing. At the same time, an effect of ITPK1 deficiency was not observed in a reductionist in vitro model (Fig. 3H). Conceivably this difference may be explained by a distinct role of different neutrophil killing mechanisms in vivo and in vitro. Alternatively, the protective effect of ITPK1 deletion in vivo may be dependent on another immune cell type. To determine whether neutrophils are required for the phenotype of ITPK1-deficient cancer cells, mice were depleted of either neutrophils or macrophages and then received a mixture of Ag-negative ($hHer2^-$) Ba/F3 cells, together with ITPK1-proficient sensBa/F3 cells, ITPK1-deficient sensBa/F3 cells, and ITPK1 KO sensBa/F3 cells overexpressing either WT or D295A kinase-dead ITPK1 (Fig. 5A). Analysis of target cell survival upon anti-hHer2 IgA treatment confirmed that treatment-induced killing of hHer2-expressing target cells was dependent on the presence of neutrophils but not macrophages (Fig. 5B). Notably, the phenotype of ITPK1 deletion and ITPK1 overexpression likewise depended on the

IgA or PBS, respectively. Prior to treatment, mice were injected with an equal mixture of sensBa/F3 tumor cells with the previously indicated genotypes. Dots represent individual mice. $****p < 0.0001$, unpaired, two-tailed t test. (**D**) Relative abundance of neutrophils ($CD11b^+Ly6G^+$) and macrophages ($CD11b^+F4/80^+$) recovered from the i.p. lavage of $hCD89^{+/-}$ transgenic mice or $hCD89^{-/-}$ littermates after a 6-h treatment with anti-hHer2 IgA or PBS, respectively. Prior to treatment, mice were injected with an equal mixture of sensBa/F3 tumor cells expressing either ITPK1-targeting or nontargeting sgRNA. Dots represent individual mice. $****p < 0.0001$, $**p = 0.0005$, no indication = nonsignificant, two-tailed t test. (**E**) Ratio of sensBa/F3 tumor cells expressing ITPK1-targeting sgRNA (clones 2 and 3), or sensBa/F3 tumor cells expressing both ITPK1-targeting sgRNA (clone 2) and ITPK1 OE, over sensBa/F3 tumor cells expressing nontargeting sgRNA (NT, clone 2) recovered from $hCD89^{+/-}$ transgenic mice or $hCD89^{-/-}$ littermates after a 16-h treatment with anti-hHer2 IgA or PBS, respectively. Prior to treatment, mice were injected with an equal mixture of sensBa/F3 tumor cells with the previously indicated genotypes. $****p < 0.0001$, $***p = 0.0002$, no indication = nonsignificant, one-way ANOVA. (**F**) Ratio of sensBa/F3 tumor cells expressing ITPK1-targeting sgRNA (clone 2) over sensBa/F3 tumor cells expressing nontargeting sgRNA (NT, clone 2) recovered from $hCD89^{+/-}$ transgenic mice after 16-h treatment with anti-hHer2 IgA, anti-hHer2 IgG1, mIgG2a isotype, or PBS, respectively. Prior to treatment, mice were injected with an equal mixture of sensBa/F3 tumor cells with the previously indicated genotypes. Dots represent individual mice. $****p < 0.0001$, no indication = nonsignificant, one-way ANOVA. (**G**) Ratio of CD47-reconstituted sensBa/F3 tumor cells expressing ITPK1-targeting sgRNA (clone 2) over CD47-reconstituted sensBa/F3 tumor cells expressing nontargeting sgRNA (NT, clone 2) recovered from $hCD89^{+/-}$ transgenic mice after a 16-h treatment with anti-hHer2 IgA, anti-hHer2 IgG1, mIgG2a isotype, or PBS, respectively. Prior to treatment, mice were injected with an equal mixture of sensBa/F3 tumor cells with the previously indicated genotypes. Dots represent individual mice. $****p < 0.0001$, no indication = nonsignificant, one-way ANOVA. (**H**) Sensitivity of WT (Ag-negative) Ba/F3 cells and sensBa/F3 cells expressing either nontargeting sgRNA (NT clone 2) or ITPK1-targeting sgRNA (clone 2), treated with the indicated concentrations of anti-hHer2 IgA, to bone marrow–derived mouse neutrophils in vitro at a 40:1 E:T ratio, as assessed by ^{51}Cr-release assay. Dots represent mean of three technical replicates. $*p = 0.0029$, two-way ANOVA. (**I**) Sensitivity of $hHer2^+$ $Cas9^+$ K562 cells expressing either nontargeting sgRNA or ITPK1-targeting sgRNA, treated with the indicated concentrations of anti-hHer2 IgA, to peripheral blood–derived human neutrophils (two separate donors) in vitro at a 40:1 E:T ratio, as assessed by ^{51}Cr-release assay. Dots represent mean of three technical replicates. $*p = 0.0136, 0.0333$, two-way ANOVA.

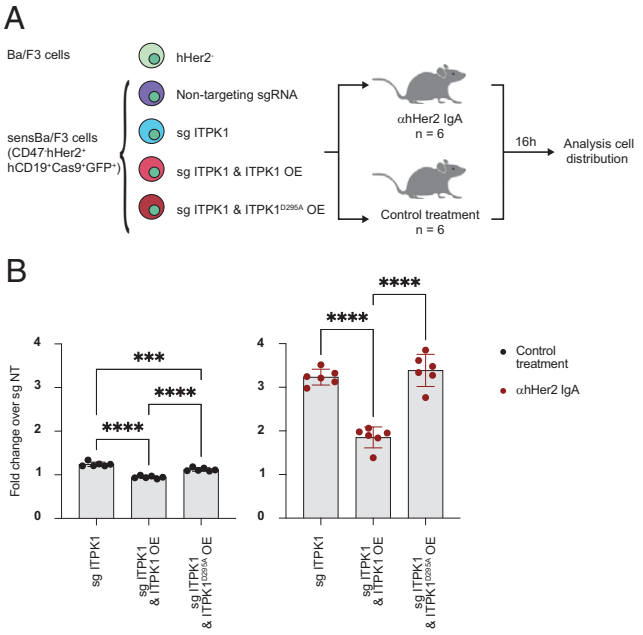

FIGURE 4. ITPK1-linked cancer cell sensitivity requires an intact ATP-binding grasp. (**A**) Schematic overview of experimental setup. A total of 2.5×10^7 WT (Ag-negative) Ba/F3 cells, sensBa/F3 cells expressing either nontargeting sgRNA (NT clone 2) or ITPK1-targeting sgRNA (clone 2), and sensBa/F3 cells expressing ITPK1-targeting sgRNA (clone 2) reconstituted with WT ITPK1 or with kinase-dead (D295A) ITPK1 were labeled and injected as mixtures into hCD89$^{+/-}$ transgenic mice or hCD89$^{-/-}$ littermates at an equal ratio. The hCD89$^{+/-}$ transgenic mice and hCD89$^{-/-}$ littermates were subsequently treated with anti-hHer2 IgA and PBS (control treatment), respectively. After 16 h, mice were sacrificed, and relative abundance of each target cell line was analyzed using flow cytometry. (**B**) Ratio of the aforementioned target cell lines over sensBa/F3 cells expressing nontargeting sgRNA in anti-hHer2 IgA and PBS-treated mice, respectively. Dots represent individual mice. ****$p < 0.0001$, ***$p = 0.0005$, no indication = nonsignificant, one-way ANOVA.

presence of neutrophils and was not influenced by the presence or absence of macrophages (Fig. 5C, 5D, Supplemental Fig. 4C). Together, these data indicate that ITPK1 deletion provides protection against IgA-induced cell killing in vivo in a process in which neutrophils are the crucial effector cells.

Pooled in vivo epistasis screen reveals an epistatic relationship between ITPK1 and IPMK

In an effort to understand possible epistatic relationships between ITPK1 and cell death–related proteins in IgA-mediated killing by neutrophils, we performed a subgenome epistasis screen (Supplemental Fig. 5A) that targeted positive regulators of cell death in both ITPK1-deficient and ITPK1-proficient sensBa/F3 cells. Specifically, ITPK1-deficient and -proficient sensBa/F3 cells were modified with an sgRNA library targeting 76 genes associated with apoptosis, necroptosis, ferroptosis, pyroptosis, and cytokine-induced cell death (30, 36, 39). Resulting sensBa/F3 libraries were injected as a mixture into hCD89-transgenic mice that received either anti-hHer2 IgA or control treatment. At 16 h postinjection, ITPK1-deficient and ITPK1-proficient sensBa/F3 cells tumor cells were isolated, and sgRNA distributions were analyzed (Supplemental Fig. 5B). Upon anti-hHer2 IgA treatment, sgRNAs that target genes sharing an epistatic relationship with ITPK1 are expected to deplete or enrich in ITPK1-proficient sensBa/F3 cells, but not in ITPK1-deficient sensBa/F3 cells. Two observations were most prominent from this epistasis screen. First, ITPK1-targeting sgRNAs were enriched in ITPK1-proficient sensBa/F3 cells but not in ITPK1-deficient sensBa/F3 cells (Supplemental Fig. 5B), confirming the validity of the genetic screen. Second, sgRNAs that target IPMK, an enzyme previously suggested to act upstream of ITPK1 in different cell types (36, 40), were likewise shown to be selectively enriched in ITPK1-proficient sensBa/F3 cells (Supplemental Fig. 5B). Together, these data provide evidence for an IPMK-ITPK1 pathway in IgA-induced target cell death.

Discussion

Neutrophils are the most abundant immune cell type in the circulation (11) and have the ability to swarm to tumor sites, where they can induce tumor cell killing upon signaling through activating Fc receptors (7, 17, 41, 42). On the basis of these observations, a number of research groups have developed IgA Abs targeting tumor-associated Ags with the aim to leverage neutrophils and their cytotoxic abilities as effector cells in cancer (43). However, our current understanding of the cellular determinants that influence cancer cell sensitivity to neutrophil activity is limited. Furthermore, the observation that neutrophils may kill target cells through a series of distinct effector mechanisms (18, 32–34) complicates the design of genetic screening approaches to identify such determinants in vitro.

With the aim to identify physiologically relevant genetic targets that influence the sensitivity of tumor cells to IgA-induced killing, we designed an in vivo pooled genetic screening strategy. As a technical proof of concept, we first demonstrated the protective effect of expression of the CD47 myeloid checkpoint ligand on a small fraction of cells among an excess of CD47-deficient counterparts in IgA-treated mice (Fig. 1). Using this model system, we subsequently performed pooled CRISPR Cas9 screens, thereby revealing ITPK1 as a sensitizer to IgA-induced and neutrophil-dependent cancer cell killing (Fig. 2). In addition, we demonstrate that this protective effect is observed in vivo but not in vitro (Fig. 3H, 3I), underscoring the importance of physiologically relevant systems for target discovery. Together, with the observation that in vivo neutrophil depletion mitigates the protective effect of ITPK1 deletion, we propose that the observed phenotype relies on the interaction of neutrophils with other cells or cytokines that are only present in vivo. Furthermore, consistent with the role of CD47 as an inhibitory receptor, we show that the ITPK1 phenotype is enhanced by but not strictly dependent on CD47 deficiency (Fig. 3F, 3G). The sensitivity of tumor cells to IgA-induced killing was partially but not fully restored upon overexpression of ITPK1 cDNA (Fig. 3E, 4B), an observation that may be explained by either missing transcript variants, supraphysiological expression levels (Supplemental Fig. 3A), or irreversible cell changes caused by ITPK1 deletion. Importantly, as overexpression of the kinase-dead D295A ITPK1 coding sequence in ITPK1 KO cells did not restore target cell sensitivity (Fig. 4B), we propose that the effect of ITPK1 on IgA-mediated neutrophil sensitivity is tied to its kinase activity. ITPK1 and IPMK have been shown in prior work to regulate TNF-α–mediated necroptosis of human cancer cell lines in vitro through the generation of inositol phosphates in a pathway that also requires receptor interacting serine/threonine kinase 3 and MLKL (36). With the caveat that differences in MLKL activation pathways have been reported between human and mice (44, 45), it seems possible that ITPK1 regulates target cell sensitivity to neutrophil attack by altering cell death pathway execution. In an effort to investigate which cell death pathway may be influenced by ITPK1 deletion, we performed a subgenome-wide CRISPR screen, targeting genes associated with a variety of cell death pathways, in sensBa/F3 cells deficient of ITPK1 (Supplemental Fig. 5A). Although our analysis did not pinpoint a specific cell death pathway that is affected by ITPK1 deletion, the data do provide evidence for an epistatic relationship between ITPK1 and IPMK. (Supplemental Fig. 5B).

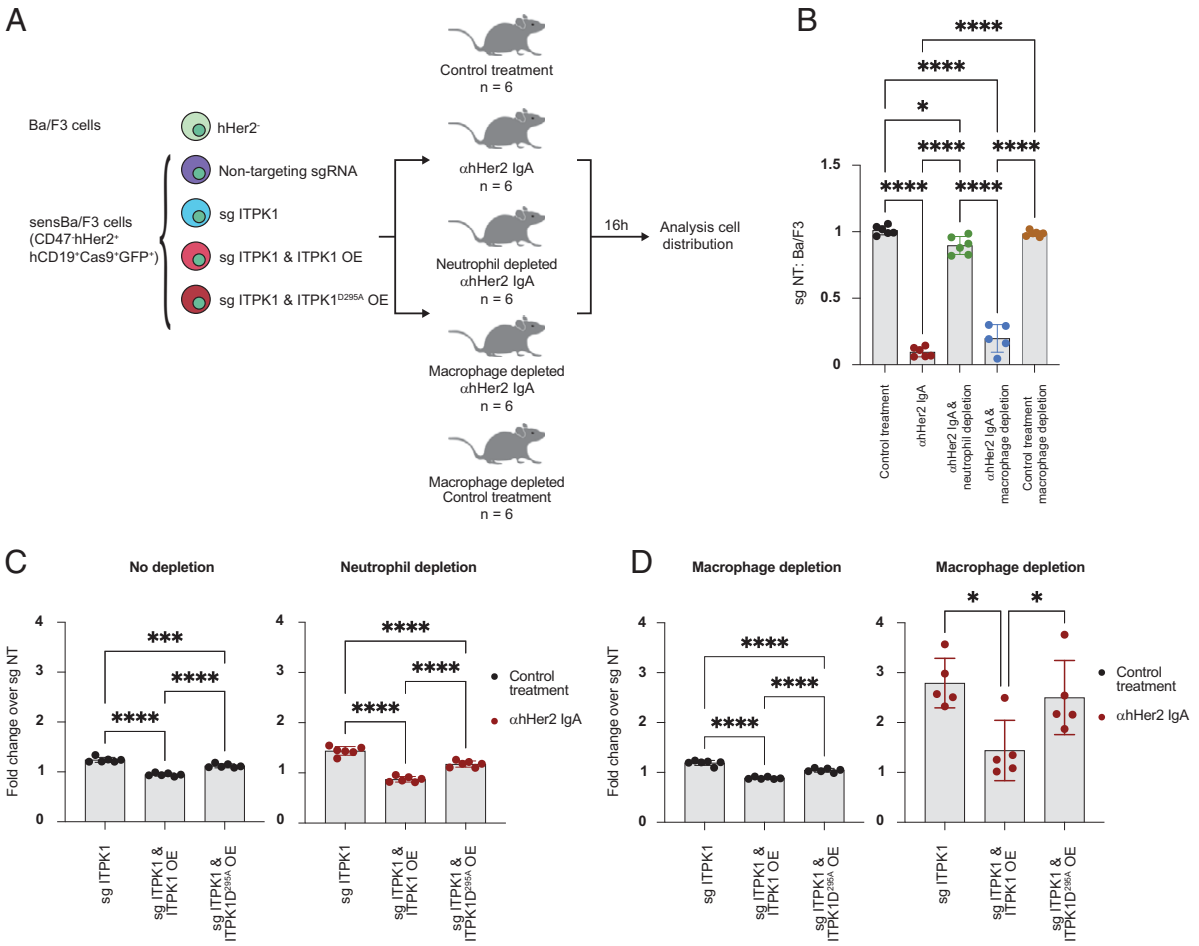

FIGURE 5. ITPK1-linked cancer cell sensitivity depends on neutrophils. (**A**) Schematic overview of experimental setup. A total of 2.5×10^7 WT (Ag-negative) Ba/F3 cells, sensBa/F3 cells expressing either nontargeting sgRNA (NT clone 2) or ITPK1-targeting sgRNA (clone 2), and sensBa/F3 cells expressing ITPK1-targeting sgRNA (clone 2) reconstituted with WT ITPK1 or with kinase-dead (D295A) ITPK1 were labeled and injected as equal mixtures into hCD89$^{+/-}$ transgenic mice, hCD89$^{+/-}$ transgenic mice pretreated with anti-Ly-6G (neutrophil depletion), hCD89$^{+/-}$ transgenic mice pretreated with chlodronate (macrophage depletion), or hCD89$^{-/-}$ littermates. Directly after tumor cell injection, hCD89$^{+/-}$ transgenic mice and hCD89$^{-/-}$ littermates were treated with anti-hHer2 IgA or PBS (control treatment), respectively. After 16 h, mice were sacrificed, and the relative abundance of each target cell line was analyzed using flow cytometry. (**B**) Ratio of sensBa/F3 cells expressing nontargeting sgRNA over WT Ba/F3 cells in each treatment group. Dots represent individual values. ****$p < 0.0001$, *$p = 0.0177$, no indication = nonsignificant, one-way ANOVA. (**C**) Ratio of cell populations described in (A) over sensBa/F3 cells expressing nontargeting sgRNA in PBS-treated mice without immune cell depletion (equivalent to Fig. 4B) or in anti-hHer2 IgA-treated mice depleted of neutrophils. Dots represent individual mice. ****$p < 0.0001$, ***$p = 0.0005$, one-way ANOVA. (**D**) Ratio of cell populations described in (A) over sensBa/F3 cells expressing nontargeting sgRNA in macrophage-depleted mice treated with PBS or with anti-hHer2 IgA. Dots represent individual mice. ****$p < 0.0001$, ***$p = 0.0005$, *$p = 0.0129$ (sg ITPK1 versus sg ITPK1 and ITPK1 OE), 0.0481 (sg ITPK1 and ITPK1 OE versus sg ITPK1 and ITPK1^{D295A} OE), one-way ANOVA.

Interestingly, next to ITPK1, we identified FERMT3 as a negative regulator of neutrophil cytotoxicity (Fig. 2C, 2E, Supplemental Fig. 2A). FERMT3 has previously been shown (46, 47) to be required for CD11b/CD18 integrin activation in neutrophils, which in turn potentiates Ab-dependent trogoptosis, and the present data suggest that integrin activation at the target cell side may likewise influence the outcome of neutrophil–target cell interactions (35, 43, 44). In future work, we speculate that the in vivo screening approach described in this study may be used to uncover additional regulators of tumor cell sensitivity to neutrophil-mediated attack.

We acknowledge the following limitations of the present work. First, although treatment with IgA leads to marked target cell depletion (Fig. 1C, 1E, 2B, 2D) and robust neutrophil infiltration (Fig. 1B, 3B, 3D), treatment with IgG Abs only results in very modest effect sizes (Supplemental Fig. 3G, 3H). Because of this, the present data do not address the possible impact of ITPK1 deletion on IgG-dependent target cell killing. Second, to assess in vivo target cell killing, we have employed an in vivo competition approach that yields highly consistent data. As a downside, the presence of multiple genotypes within the same animal precludes an analysis of indirect effects of any of the coadministered genotypes on, for example, immune cell infiltrate. Finally, although the data obtained point toward a critical role for neutrophils in the observed in vivo target cell killing, it remains to be elucidated why the protective effect of ITPK1 deficiency is only apparent in vivo and not in vitro. On a more general note, recent work has demonstrated that the activity of (T cell–based) cancer immunotherapies can depend on accumulation and activation of intratumoral neutrophils (48). The genetic screening approach described in this study should provide a means to better dissect the mechanisms that control such neutrophil-mediated antitumor activity.

Disclosures

The authors have no financial conflicts of interest.

References

1. Reff, M. E., K. Carner, K. S. Chambers, P. C. Chinn, J. E. Leonard, R. Raab, R. A. Newman, N. Hanna, and D. R. Anderson. 1994. Depletion of B cells in vivo by a chimeric mouse human monoclonal antibody to CD20. *Blood* 83: 435–445.
2. Smith, M. R. 2003. Rituximab (monoclonal anti-CD20 antibody): mechanisms of action and resistance. *Oncogene* 22: 7359–7368.
3. Hudis, C. A. 2007. Trastuzumab—mechanism of action and use in clinical practice. *N. Engl. J. Med.* 357: 39–51.
4. Petricevic, B., J. Laengle, J. Singer, M. Sachet, J. Fazekas, G. Steger, R. Bartsch, E. Jensen-Jarolim, and M. Bergmann. 2013. Trastuzumab mediates antibody-dependent cell-mediated cytotoxicity and phagocytosis to the same extent in both adjuvant and metastatic HER2/neu breast cancer patients. *J. Transl. Med.* 11: 307.
5. Musolino, A., W. J. Gradishar, H. S. Rugo, J. L. Nordstrom, E. P. Rock, F. Arnaldez, and M. D. Pegram. 2022. Role of Fcγ receptors in HER2-targeted breast cancer therapy. *J. Immunother. Cancer* 10: e003171.
6. Lin, T. 2010. Ofatumumab: a novel monoclonal anti-CD20 antibody. *Pharmgenomics Pers. Med.* 3: 51–59.
7. Brandsma, A. M., S. Bondza, M. Evers, R. Koutstaal, M. Nederend, J. H. M. Jansen, T. Rösner, T. Valerius, J. H. W. Leusen, and T. Ten Broeke. 2019. Potent Fc receptor signaling by IgA leads to superior killing of cancer cells by neutrophils compared to IgG. *Front. Immunol.* 10: 704.
8. Koernig, S., I. K. Campbell, C. Mackenzie-Kludas, A. Schaub, M. Loetscher, W. Ching Ng, R. Zehnder, P. Pelczar, I. Sanli, M. Alhamdoosh, et al. 2019. Topical application of human-derived Ig isotypes for the control of acute respiratory infection evaluated in a human CD89-expressing mouse model. *Mucosal Immunol.* 12: 1013–1024.
9. Hansen, I. S., W. Hoepel, S. A. J. Zaat, D. L. P. Baeten, and J. den Dunnen. 2017. Serum IgA immune complexes promote proinflammatory cytokine production by human macrophages, monocytes, and Kupffer cells through FcαRI-TLR cross-talk. *J. Immunol.* 199: 4124–4131.
10. Boross, P., S. Lohse, M. Nederend, J. H. M. Jansen, G. van Tetering, M. Dechant, M. Peipp, L. Royle, L. P. Liew, L. Boon, et al. 2013. IgA EGFR antibodies mediate tumour killing in vivo. *EMBO Mol. Med.* 5: 1213–1226.
11. Coffelt, S. B., M. D. Wellenstein, and K. E. de Visser. 2016. Neutrophils in cancer: neutral no more. *Nat. Rev. Cancer* 16: 431–446.
12. Taylor, B. C., and J. M. Balko. 2022. Mechanisms of MHC-I downregulation and role in immunotherapy response. *Front. Immunol.* 13: 844866.
13. Kalbasi, A., and A. Ribas. 2020. Tumour-intrinsic resistance to immune checkpoint blockade. *Nat. Rev. Immunol.* 20: 25–39.
14. Ibáñez-Molero, S., A. van Vliet, J. Pozniak, K. Hummelink, A. M. Terry, K. Monkhorst, J. Sanders, I. Hofland, E. Landeloos, Y. Van Herck, et al. 2022. SERPINB9 is commonly amplified and high expression in cancer cells correlates with poor immune checkpoint blockade response. *Oncoimmunology* 11: 2139074.
15. van Spriel, A. B., J. H. W. Leusen, M. van Egmond, H. B. P. M. Dijkman, K. J. M. Assmann, T. N. Mayadas, and J. G. J. van de Winkel. 2001. Mac-1 (CD11b/CD18) is essential for Fc receptor–mediated neutrophil cytotoxicity and immunologic synapse formation. *Blood* 97: 2478–2486.
16. Zhao, X. W., E. M. van Beek, K. Schornagel, H. Van der Maaden, M. Van Houdt, M. A. Otten, P. Finetti, M. Van Egmond, T. Matozaki, G. Kraal, et al. 2011. CD47-signal regulatory protein-α (SIRPα) interactions form a barrier for antibody-mediated tumor cell destruction. *Proc. Natl. Acad. Sci. U. S. A.* 108: 18342–18347.
17. Behrens, L. M., T. K. van den Berg, and M. van Egmond. 2022. Targeting the CD47-SIRPα innate immune checkpoint to potentiate antibody therapy in cancer by neutrophils. *Cancers (Basel)* 14: 3366.
18. Treffers, L. W., T. Ten Broeke, T. Rösner, J. H. M. Jansen, M. van Houdt, S. Kahle, K. Schornagel, P. J. J. H. Verkuijlen, J. M. Prins, K. Franke, et al. 2020. IgA-mediated killing of tumor cells by neutrophils is enhanced by CD47-SIRPα checkpoint inhibition. *Cancer Immunol. Res.* 8: 120–130.
19. van Egmond, M., A. J. van Vuuren, H. C. Morton, A. B. van Spriel, L. Shen, F. M. Hofhuis, T. Saito, T. N. Mayadas, J. S. Verbeek, and J. G. van de Winkel. 1999. Human immunoglobulin A receptor (FcalphaRI, CD89) function in transgenic mice requires both FcR gamma chain and CR3 (CD11b/CD18). *Blood* 93: 4387–4394.
20. Stip, M. C., J. H. M. Jansen, M. Nederend, M. Tsioumpekou, M. Evers, P. A. Olofsen, F. Meyer-Wentrup, and J. H. W. Leusen. 2023. Characterization of human Fc alpha receptor transgenic mice: comparison of CD89 expression and antibody-dependent tumor killing between mouse strains. *Cancer Immunol. Immunother.* 72: 3063–3077.
21. Logtenberg, M. E. W., J. H. M. Jansen, M. Raaben, M. Toebes, K. Franke, A. M. Brandsma, H. L. Matlung, A. Fauster, R. Gomez-Eerland, N. A. M. Bakker, et al. 2019. Glutaminyl cyclase is an enzymatic modifier of the CD47-SIRPα axis and a target for cancer immunotherapy. *Nat. Med.* 25: 612–619.
22. Gibson, D. G., L. Young, R.-Y. Chuang, J. C. Venter, C. A. Hutchison, and H. O. Smith. 2009. Enzymatic assembly of DNA molecules up to several hundred kilobases. *Nat. Methods* 6: 343–345.
23. Bracke, M., J. W. Lammers, P. J. Coffer, and L. Koenderman. 2001. Cytokine-induced inside-out activation of FcalphaR (CD89) is mediated by a single serine residue (S263) in the intracellular domain of the receptor. *Blood* 97: 3478–3483.
24. Brinkman, E. K., T. Chen, M. Amendola, and B. van Steensel. 2014. Easy quantitative assessment of genome editing by sequence trace decomposition. *Nucleic Acids Res.* 42: e168.
25. Murakami, A., M. Maekawa, K. Kawai, J. Nakayama, N. Araki, K. Semba, T. Taguchi, Y. Kamei, Y. Takada, and S. Higashiyama. 2019. Cullin-3/KCTD10 E3 complex is essential for Rac1 activation through RhoB degradation in human epidermal growth factor receptor 2-positive breast cancer cells. *Cancer Sci.* 110: 650–661.
26. Culibrk, L., C. A. Croft, A. Toor, S. J. Yang, G. K. Singhera, D. R. Dorscheid, M. M. Moore, and S. J. Tebbutt. 2019. Phagocytosis of *Aspergillus fumigatus* by human bronchial epithelial cells is mediated by the Arp2/3 complex and WIPF2. *Front. Cell. Infect. Microbiol.* 9: 16.
27. Li, W., H. Xu, T. Xiao, L. Cong, M. I. Love, F. Zhang, R. A. Irizarry, J. S. Liu, M. Brown, and X. S. Liu. 2014. MAGeCK enables robust identification of essential genes from genome-scale CRISPR/Cas9 knockout screens. *Genome Biol.* 15: 554.
28. Aleksander, S. A., J. Balhoff, S. Carbon, J. M. Cherry, H. J. Drabkin, D. Ebert, M. Feuermann, P. Gaudet, N. L. Harris, D. P. Hill, et al. Gene Ontology Consortium. 2023. The Gene Ontology knowledgebase in 2023. *Genetics* 224: iyad031.
29. Ashburner, M., C. A. Ball, J. A. Blake, D. Botstein, H. Butler, J. M. Cherry, A. P. Davis, K. Dolinski, S. S. Dwight, J. T. Eppig, et al. 2000. Gene Ontology: tool for the unification of biology. *Nat. Genet.* 25: 25–29.
30. Hitomi, J., D. E. Christofferson, A. Ng, J. Yao, A. Degterev, R. J. Xavier, and J. Yuan. 2008. Identification of a molecular signaling network that regulates a cellular necrotic cell death pathway. *Cell* 135: 1311–1323.
31. Gruijs, M., C. A. N. Sewnath, and M. van Egmond. 2021. Therapeutic exploitation of neutrophils to fight cancer. *Semin. Immunol.* 57: 101581.
32. Amulic, B., C. Cazalet, G. L. Hayes, K. D. Metzler, and A. Zychlinsky. 2012. Neutrophil function: from mechanisms to disease. *Annu. Rev. Immunol.* 30: 459–489.
33. Dallegri, F., L. Ottonello, A. Ballestrero, P. Dapino, F. Ferrando, F. Patrone, and C. Sacchetti. 1991. Tumor cell lysis by activated human neutrophils: analysis of neutrophil-delivered oxidative attack and role of leukocyte function-associated antigen 1. *Inflammation* 15: 15–30.
34. Matlung, H. L., L. Babes, X. W. Zhao, M. van Houdt, L. W. Treffers, D. J. van Rees, K. Franke, K. Schornagel, P. Verkuijlen, H. Janssen, et al. 2018. Neutrophils kill antibody-opsonized cancer cells by trogoptosis. *Cell Rep.* 23: 3946–3959.e6.
35. Xiong, S., L. Dong, and L. Cheng. 2021. Neutrophils in cancer carcinogenesis and metastasis. *J. Hematol. Oncol.* 14: 173.
36. Dovey, C. M., J. Diep, B. P. Clarke, A. T. Hale, D. E. McNamara, H. Guo, N. W. Brown, J. Y. Cao, C. R. Grace, P. J. Gough, et al. 2018. MLKL Requires the inositol phosphate code to execute necroptosis. *Mol. Cell* 70: 936–948.e7.
37. Chamberlain, P. P., X. Qian, A. R. Stiles, J. Cho, D. H. Jones, S. A. Lesley, E. A. Grabau, S. B. Shears, and G. Spraggon. 2007. Integration of inositol phosphate signaling pathways via human ITPK1. *J. Biol. Chem.* 282: 28117–28125.
38. Qian, X., J. Mitchell, S.-J. Wei, J. Williams, R. M. Petrovich, and S. B. Shears. 2005. The Ins(1,3,4)P3 5/6-kinase/Ins(3,4,5,6)P4 1-kinase is not a protein kinase. *Biochem. J.* 389: 389–395.
39. Galluzzi, L., I. Vitale, S. A. Aaronson, J. M. Abrams, D. Adam, P. Agostinis, E. S. Alnemri, L. Altucci, I. Amelio, D. W. Andrews, et al. 2018. Molecular mechanisms of cell death: recommendations of the Nomenclature Committee on Cell Death 2018. *Cell Death Differ.* 25: 486–541.
40. Desfougères, Y., M. S. C. Wilson, D. Laha, G. J. Miller, and A. Saiardi. 2019. ITPK1 mediates the lipid-independent synthesis of inositol phosphates controlled by metabolism. *Proc. Natl. Acad. Sci. U. S. A.* 116: 24551–24561.
41. Bakema, J. E., S. H. Ganzevles, D. M. Fluitsma, M. W. Schilham, R. H. J. Beelen, T. Valerius, S. Lohse, M. J. Glennie, J. P. Medema, and M. van Egmond. 2011. Targeting FcαRI on polymorphonuclear cells induces tumor cell killing through autophagy. *J. Immunol.* 187: 726–732.
42. Otten, M. A., J. E. Bakema, C. W. Tuk, M. J. Glennie, A. L. Tutt, R. H. J. Beelen, J. G. J. van de Winkel, and M. van Egmond. 2012. Enhanced FcαRI-mediated neutrophil migration towards tumour colonies in the presence of endothelial cells. *Eur. J. Immunol.* 42: 1815–1821.
43. van Tetering, G., M. Evers, C. Chan, M. Stip, and J. Leusen. 2020. Fc engineering strategies to advance IgA antibodies as therapeutic agents. *Antibodies* 9: 70.
44. Davies, K. A., M. C. Tanzer, M. D. W. Griffin, Y. F. Mok, S. N. Young, R. Qin, E. J. Petrie, P. E. Czabotar, J. Silke, and J. M. Murphy. 2018. The brace helices of MLKL mediate interdomain communication and oligomerisation to regulate cell death by necroptosis. *Cell Death Differ.* 25: 1567–1580.
45. Murphy, J. M., P. E. Czabotar, J. M. Hildebrand, I. S. Lucet, J.-G. Zhang, S. Alvarez-Diaz, R. Lewis, N. Lalaoui, D. Metcalf, A. I. Webb, et al. 2013. The pseudokinase MLKL mediates necroptosis via a molecular switch mechanism. *Immunity* 39: 443–453.
46. Bouti, P., X. W. Zhao, P. J. J. H. Verkuijlen, A. T. J. Tool, M. van Houdt, N. Köker, M. Y. Köker, O. Keskin, S. Akbayram, R. van Bruggen, et al. 2021. Kindlin3-dependent CD11b/CD18-integrin activation is required for potentiation of neutrophil cytotoxicity by CD47–SIRPα checkpoint disruption. *Cancer Immunol. Res.* 9: 147–155.
47. Bouti, P., S. D. S. Webbers, S. C. Fagerholm, R. Alon, M. Moser, H. L. Matlung, and T. W. Kuijpers. 2020. β2 integrin signaling cascade in neutrophils: more than a single function. *Front. Immunol.* 11: 619925.
48. Gungabeesoon, J., N. A. Gort-Freitas, M. Kiss, E. Bolli, M. Messemaker, M. Siwicki, M. Hicham, R. Bill, P. Koch, C. Cianciaruso, et al. 2023. A neutrophil response linked to tumor control in immunotherapy. *Cell* 186: 1448–1464.e20.